

Application of a Wind Model for the El Paso–Juarez Airshed

Roderick Pearson and Rosa Fitzgerald

Physics Department, University of Texas, El Paso

ABSTRACT

A time-dependent, 3-dimensional mesoscale model, version 5 (MM5), developed by the Penn State University and the National Center for Atmospheric Research, was applied to study the meteorology over complex terrain of the El Paso–Juarez area. MM5 meteorological output data were compared against experimental data from the Texas Natural Resource Conservation Commission on days of reported high ozone concentrations. Model runs were conducted for a 36-, 12-, 4-km grid arrangement. Results indicate that the dispersion of pollutants by wind plays a significant role on days of low peak ozone concentration.

INTRODUCTION

The El Paso, TX, metropolitan area is concentrated along the northeastern bank of the Rio Grande river in the Paso del Norte region (Figure 1). The city extends northward east of the Franklin Mountains toward the Tularosa Bolson as well as west–northwest toward New Mexico along the west side of the Franklin Mountains. Ciudad Juarez, Mexico, is located immediately across the river from El Paso, forming a contiguous metropolitan area of approximately 2 million people separated by the political boundary between the United States and Mexico. The elevation of the metropolitan areas is ~1200 m. The mountains in the region are oriented north–south. The Franklin Mountains

start ~20 km north of El Paso and extend northward ~40 km with an elevation of 2200 m. The nearly cone-shaped Juarez Mountain is located ~30 km south of Juarez with an elevation of 1600 m. Three major mountain ranges are located about 100–200 km from the El Paso–Juarez airshed (EPJA): the Sacramento Mountains to the east, the Rocky Mountains to the north, and the Santa Maria Mountains to the south. The elevations of these mountains are 2000–4000 m.

The El Paso area has been labeled by the U.S. Environmental Protection Agency (EPA) as being in nonattainment of the National Ambient Air Quality Standard for ozone. Nonattainment means that measured ozone levels in the region have been higher than 125 parts per billion (ppb) for 3 days within a 3-year period. A major need in the EPJA is an investigation of the causes of elevated ozone concentrations. Results of such an investigation will be used to develop and evaluate effective emission control strategies. As part of this effort, the EPA, the Texas Natural Resource Conservation Committee (TNRCC), and other government and private agencies, in coordination with the Mexican Instituto Nacional de Ecología, conducted the Paso Del Norte Ozone Study (PDNOS) during the summers of 1996 and 1997.¹ In addition, emission inventory development activities have intensified, and applications of air quality models to the region are planned. During the PDNOS, surface meteorology and air quality were monitored at 22 stations, and upper air meteorology was monitored at four stations using two Windprofilers, one SODAR, and one Rawindsonde. In addition, both meteorology and air quality were monitored from aircraft.

The meteorological model MM5 was selected for this study. MM5 is a 3-dimensional, limited-area primitive equation model developed by the Penn State University and the National Center for Atmospheric Research.² The model is based on the prognostic equations for 3-dimensional wind components (u , v , w), temperature (T), the water vapor mixing ratio (qv), and the perturbation pressure (p'). It uses a constant reference-state pressure to increase the accuracy of calculations in the vicinity of steep terrain. The model equations are solved using an efficient

IMPLICATIONS

Many parts of the world with an air quality problem, such as the El Paso–Juarez airshed (EPJA), do not have a comprehensive database to establish source-receptor relationships. A comprehensive model like MM5 can be used effectively to obtain such a database to study regional meteorological conditions leading to high ozone concentrations. The details of the information obtained from the model depend on the model physics, grid resolution, and details of the model inputs. Model accuracy can be greatly improved with improved model inputs. In the El Paso–Juarez case, the model provided information for the data void areas. In addition, since the MM5 model has never been used in this area, this research will provide a framework for future meteorological studies, which will enable an enhanced analysis of the fate and transport of pollutants.

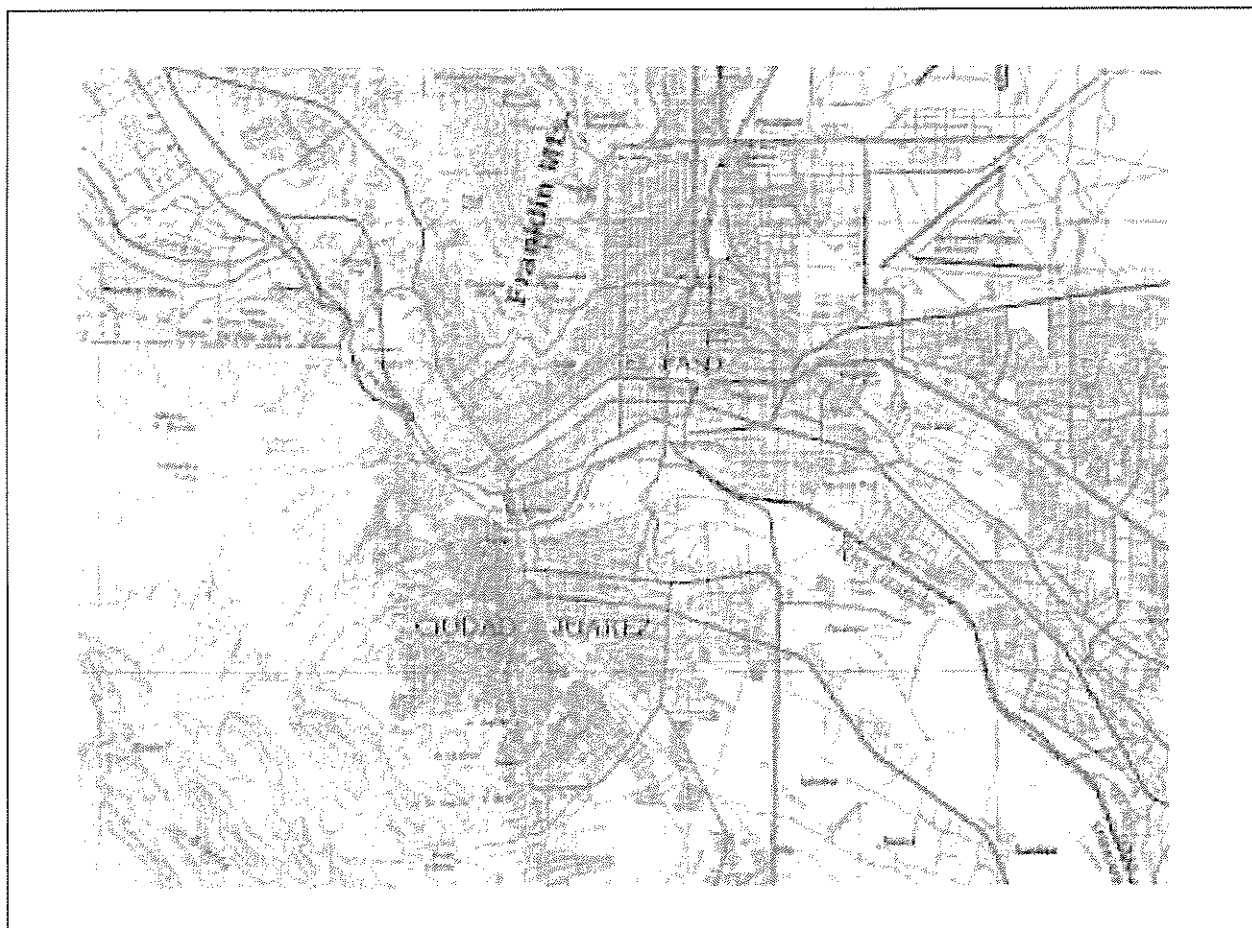


Figure 1. Map of El Paso–Juarez.

split semi-implicit temporal integration scheme. It also has a nested-grid capability of nine different domains of arbitrary horizontal and vertical resolutions. The nested grid interfaces can be either one-way or two-way interactive. The vertical coordinate of the model is a terrain-following non-dimensionalized pressure coordinate. MM5 is an advanced prognostic wind model, constantly evolving by the contributions of worldwide researchers. It has the capability of 4-dimensional data assimilation (FDDA), and of handling complex terrain. It is also nonproprietary and compatible with most photochemical air quality models. These reasons led us to select it for the study of the EPJA.

The purpose of this study was to perform an initial evaluation of the ability of MM5 to simulate the meteorology in the EPJA. The MM5 model had never been used before in this area; furthermore, it was the first time the model was used in this area in connection with ozone studies. This research will provide inputs in subsequent air quality model applications and the understanding of the impact of the wind on the high ozone in the region. It is known¹ that some of the local meteorological

conditions leading to the formation of high ozone episodes in El Paso are

- (1) Stagnant or weak early morning surface winds. The morning surface-based mixed layer is lower and grows more slowly than on days with lower maximum ozone concentrations.
- (2) Higher surface precursor concentrations. This could be attributed to the stronger inversion associated with the slow growth of the mixed layer and lower mixing heights.
- (3) Aloft warming and the resulting increase in stability. It is believed that this is the major factor influencing the growth rate of the mixed layer.

Since MM5 allows for the calculation of a significantly larger number of meteorological variables other than wind patterns, this research will provide the necessary infrastructure to pursue more ozone studies in the future. Furthermore, subsequent work using trajectory analysis in conjunction with MM5 will allow understanding of the pollution transport in this area in order to take proper measurements to improve the air quality in the region. The results of this research will also be used for the design

of new meteorological and air quality monitoring programs in the area.

In order to better understand the impact of the wind on ozone in the region, it is necessary to determine the region's airflow features, such as the slope flows and mountain-valley circulations. The complex terrain of the EPJA introduces a variety of mesoscale effects through circulation systems that are produced by differential heating and cooling of various surfaces. The differences in meteorological conditions on the east and west sides of the mountains and in the upper and lower valleys may play an important role in the transport of ozone. For example, the west side of the mountains and the upper valley are subject to mountain-valley flows affected by the average higher humidity of the upper valley and the lower humidity of the mountains. This section also sees higher rainfall totals than other parts of the area. The east side of the mountains is influenced by a large heat island effect from the city and valley flow with lower mean humidity. The lower valley has a higher mean humidity than the east side of the mountain and sees valley flow but does not experience any mountain effects. Its precipitation is mainly from storms coming from the south that are deflected around the Juarez Mountains.

A key factor in ozone formation is the emission characteristics of the region. In the EPJA, the number of pollution emitters has greatly increased with the implementation of the North American Free Trade Agreement. Mobile emitters have increased with the number of private and transport vehicles in operation in the region. In the United States, this has been mitigated somewhat with the use of cleaner-burning gasoline and low-emissions requirements for vehicles. However, in Ciudad Juarez, there are no such requirements. The vehicle type that has shown the fastest growth has been the Mexican trucks and private vehicles.

Exacerbating the problem of mobile emitters is the increased traffic across the international border. Increased traffic means that a larger number of vehicles are sitting idle at the border crossing points for longer periods of time, producing large pockets of emissions. As for mobile emitters, stationary sources of emissions have grown. For example, El Paso smelting operations have increased their activities. In Ciudad Juarez, tire disposal facilities and various types of manufacturing plants have also increased their activities.

The exact increases in emissions due to increased activities have not been fully determined. Therefore, these contributions must be studied in detail. Developing effective emission control strategies requires an understanding of the relationships between emissions, meteorology, and the formation of ozone. Photochemical air quality models are used to obtain guidance for developing control strategies. Several attempts were made

for photochemical model simulations in the area using the urban airshed model.³⁻⁵ Recently, Randolph et al.⁶ and Emery et al.⁷ applied the RAMS and urban airshed models. A major component of the photochemical model is its meteorology input, which emphasizes the need for this research work using MM5.

METHODOLOGY

It was necessary to evaluate several options of the model to determine the optimum MM5 settings suitable for the EPJA. The first step was to evaluate various parameterization schemes of the model for the major physical processes. This included cloud parameterization, radiation, planetary boundary layer schemes, and the precipitation scheme. Each simulation was designed to determine the best model options to optimize results under sparse meteorological data. The schemes listed in Table 1 represent those chosen for the model simulations. The Blackadar planetary boundary layer (PBL) scheme was used for the coarse and intermediate domains. The warm rain precipitation scheme was chosen because it was the most compatible scheme among the available schemes in MM5 to represent the meteorology in the area. Three horizontal grids were chosen. The coarse grid had 36-km, the intermediate grid 12-km, and the fine grid 4-km resolutions. Table 2 gives the horizontal grid details and the nesting. Each grid was centered at 31.7 N latitude and 106.4 W longitude. Figure 2a shows the domains. Twenty-two vertical grids were selected with the following pressure levels: 1000, 999, 975, 950, 875, 850, 825, 800, 750, 725, 700, 650, 600, 550, 500, 450, 400, 350, 300, 250, 150, and 100 mb.

The terrain elevation and land use data (see Figure 2b for the 4-km domain land use data) were taken from National Center for Atmospheric Research's (NCAR)

Table 1. Schemes.

Parameterization	Scheme
Cloud development	Grell (none used in 4-km grid)
Radiation	Simple
PBL	Blackadar, Burk-Thompson
Precipitation	Warm rain

Table 2. Grid structure.

Domain	Cell Size (km)	I Number	J Number
1	36	37	37
2	12	49	49
3	4	55	55

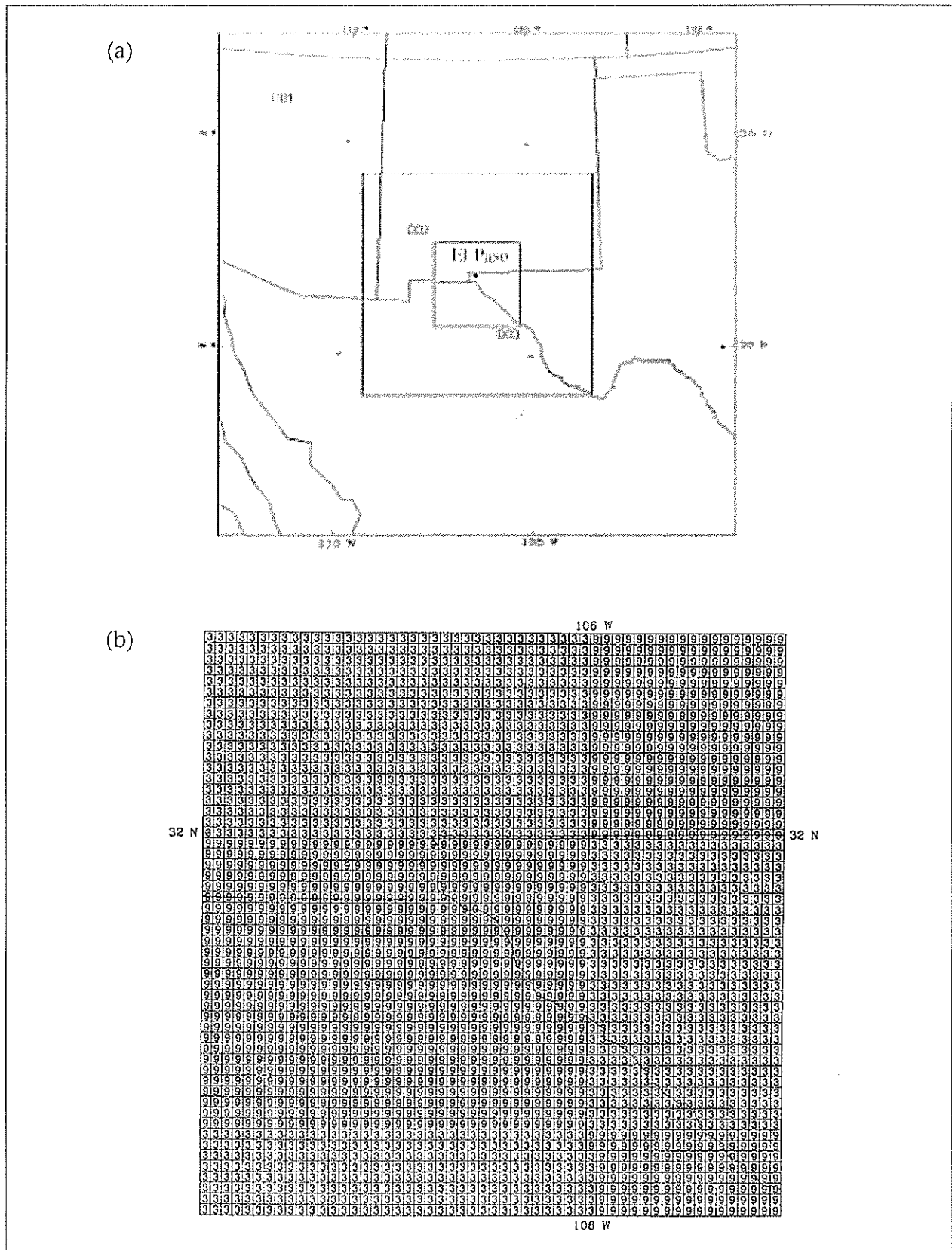


Figure 2. (a) Modeling domains. (b) Land use categorization of the 4-km domain. Each cell contains one category as determined by MM5. A "3" represents range-grassland and a "9" represents desert.

database. The 36-km grid used the 5-min GDC global data set, and the 12-km grids used the 1-min data set. The 4-km domain used the 30-arc sec topographical data from the United States Geological Survey (USGS). This data has a resolution of ~1 km. The land use data had 10-min resolution for the first two domains. The 4-km domain used the USGS-derived land use land cover database with the same resolution as the topographical data.

The variable data are the atmospheric data for cloud cover and precipitation. The atmospheric data were derived from the NMC global spectral model data assimilation system database archived at NCAR. For our area of interest, these data were the National Weather Service (NWS) twice-daily radiosondes and 3-hr surface observations. The NWS data include the horizontal wind components (u and v), temperature (T), relative humidity (RH), sea-level pressure (SLP) and ground temperature (Tg), where ground temperature is surface temperature over land and sea-surface temperature over water. The clouds and precipitation^{2,8} are calculated via the thermodynamic and cloud formulations in the model and require no input data. Each domain was initialized using the NCAR archived database.

Case studies were done on days of reported high ozone concentration, such as August 12–14, 1996, and September 3–5, 1996. Figures 3a and b show the ozone values, the area of major concentration, for August 12 and 13, 1996, at 12:00 p.m. Each MM5 simulation was started 36 hr prior to the first hour of the study (00:00 Greenwich Mean Time) to allow for spin-up time. The model was initialized as discussed above utilizing data from the aforementioned databases, except for the TNRCC data to be used later for comparison, for the days of the studies in the 4-km domain.

The prognostic portion of the model was run for the two outer domains, in two-way nest mode. In this mode, the nested domains share information across their boundary. This allows the outermost domain to receive information from the inner domain. The output was checked for validity. This was done by graphing the output of the second domain (12-km) to verify the reproduction of synoptic conditions, such as wind speed, wind direction, and temperature. The output of the second domain was used to create the initial and lateral boundary conditions for the third domain (4-km). With the boundary conditions verified, the fine grid was simulated. The fine grid output was compared directly to TNRCC data to look at flow patterns.

The sparseness of data for this region also necessitated other differences. MM5 has two distinct nudging methods, Gridded Analysis and Observational Nudging. In the first nudging method, Newtonian relaxation terms are added to the prognostic equations. These terms relax the model value toward a given analysis. The model linearly interpolates the analyses in time to determine the value toward which the model relaxes its solution. The second nudging method also uses relaxation terms, but the method is similar to objective analysis techniques where the relaxation term is based on the model error at observational stations. The relaxation is such as to reduce this error. In our calculations, FDDA gridded analysis nudging, as outlined by Stauffer and Seaman,⁹ was utilized. Wind, humidity, and temperature (excluding surface temperature) were nudged. In addition, observational nudging was also employed.

Meteorological data from 21 surface sites were used. The data included were wind speed, wind direction, and

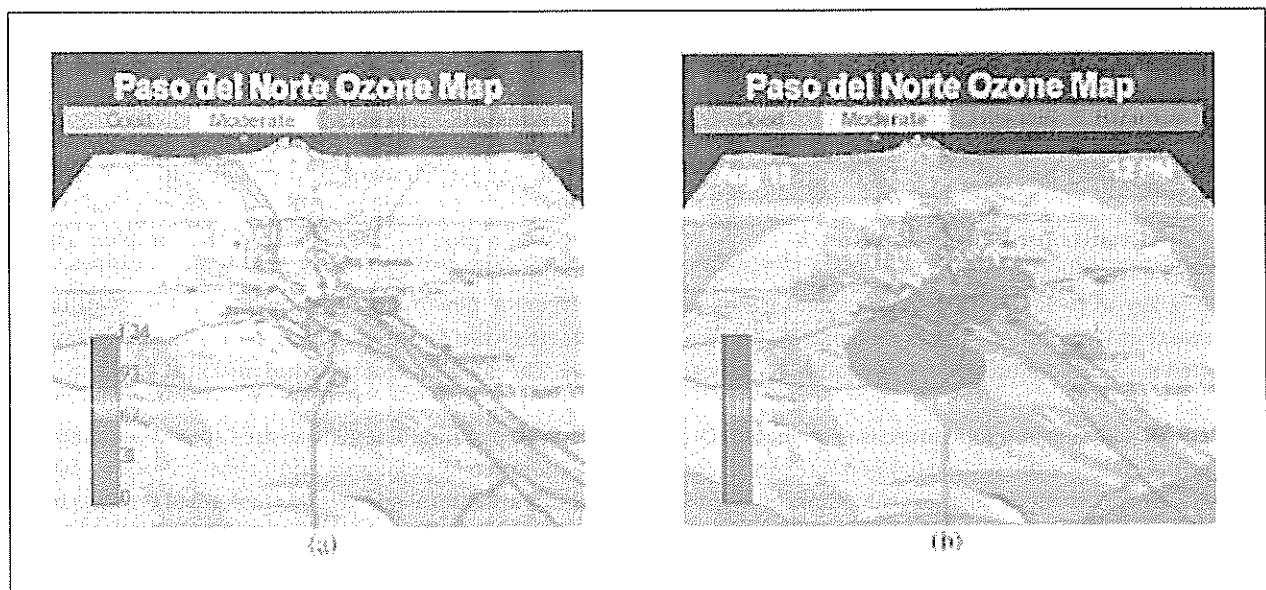


Figure 3. Ozone maps of the El Paso airshed. (a) August 12, 1996. (b) August 13, 1996.

temperature. The wind speed and wind direction were used to calculate the u and v components of the wind at each monitoring site. The u and v components were the actual wind inputs to the model. Observational nudging was done for each domain.

Previous MM5 simulations in California showed that the Blackadar PBL¹⁰ scheme had a hot bias in nightly temperature.¹¹ It did not cool the air appropriately in smaller domains. A comparison of the Blackadar and the Burk-Thompson PBL¹² schemes was also performed to investigate their impact on the simulations. The two PBL schemes were evaluated to determine their effect on model response under the situation of sparse data. These findings allowed us to best select parameters for future studies. Upon satisfactory completion of the preliminary studies, subsequent case studies were done. The case studies were conducted using the above-mentioned procedures. The September and August time periods shown in the 12-km tables used the Blackadar PBL scheme. This scheme was found to work more efficiently on the larger domains; however, the Burk-Thompson worked better for the 4-km domain.

RESULTS

The methodology described above was used to produce the results with the following information taken into account. The meteorological data from the observational sites are derived from observations taken at local monitoring sites. These sites consist of a 10-m tower with gauges to measure wind speed, wind direction, humidity, and temperature. The gauges for the wind speed and wind direction are at 10 m above ground level. The gauges for the humidity and temperature are at 8 m. The variance in the humidity and temperature at 10 and 8 m above ground level is considered to be negligible. Data from these sites were available for use. To be consistent with these data, the surface layer in the MM5 model was considered to be 10 m above ground level. This allowed direct comparison with the observed data.

Results for 12-km, Domain 2

The statistics for the two episodes are given in Tables 3a and 3b (a key to their meaning can be found in the research work by Willmott¹³). The surface temperatures were converted to Celsius for inclusion in the table, but all calculations were done in Kelvin. The model's ability to reproduce the daily mean temperature was evaluated. Our MM5 error results for the surface temperature estimation are generally consistent with other evaluations from similar studies.¹¹ In the August episode, the mean temperature increased by 0.18 °C from the first day to the second. MM5 overpredicted the first day's mean temperature but matched the second day's mean very closely. The observed

mean temperature increased by 3.63 °C from the second to the third day. This was caused by the strengthening of a 500-mb pressure ridge, just west of El Paso, extending from southern Utah. MM5 reproduced this increase to within 0.03%. The September mean temperatures show a decrease of 1.23 °C during the episode. MM5 shows a corresponding 1.5 °C decrease over the same period. A 1.05 °C decrease occurred between days 1 and 2.

The observed daily mean wind speeds show a light wind on August 12 and nearly stagnant winds on August 13, with the wind speed value doubled on August 14. MM5-predicted wind speeds show a general trend of decreasing daily mean wind speeds for the episode. More observational data were available for wind speed at the end of the episode than at the beginning. The model appears not to be strongly influenced by the observational nudging of the wind speed data, most likely due to a sparse amount of data being available during this time period. Analysis of the scalar mean u and v components for the episode demonstrate the same trend for the u component as for the mean wind speed. The September episode shows better agreement between modeled and observed data; however, there is still an overestimation by MM5. More observational data was available throughout this episode than in August. The u and v components repeat the overestimation for all days. The only exception is the mean predicted v component for September 3 is 6.5% less.

The root mean square error (RMSE) of both episodes was less than 3.0. The RMSEs for each individual monitoring site were not known specifically and need to be further examined. High RMSE values at one site influence the cumulative value to be higher. This causes the agreement between the observed and calculated data to diminish for all stations. The standard deviation of the wind speed and the u and v components are not effective measures of variability at this scale.

Results for 4-km, Domain 3

The qualitative behavior of the winds in the 4-km domain was first investigated. The general behavioral trends were well reproduced; for example, the complex terrain introduces local circulation effects. A sample is depicted in Figure 4, where horizontal winds for the August episode are shown for the 4-km domain at 10 m above ground level. The graphs are of the wind profile at 4:00 a.m. and 4:00 p.m. on August 13, 1996, showing the downslope and upslope flows. These flows are thought to dominate the transport of pollutants and ozone precursors. Subsequently, a statistical analysis was performed on the results. The statistical results are summarized for the August episode in Table 4a and for the September episode in Table 4b. For both the August and September episodes, MM5 overpredicted the mean wind speed for the entire episode.

Table 3a. Statistical summary of the August episode—Domain 2.

Performance Attribute	Aug 12, 1996	Aug 13, 1996	Aug 14, 1996	Mean
Mean wind speed (m/sec)	1.15	0.82	1.66	1.21
Mean predicted wind speed (m/sec)	2.54	1.87	1.94	2.12
Observed standard deviation	0.47	0.49	0.54	0.50
Predicted standard deviation	0.62	0.61	0.60	0.61
RMSE	2.44	2.93	1.42	2.26
RMSE _U	2.18	2.62	1.27	2.02
RMSE _S	1.09	1.31	0.64	1.01
Mean predicted U component (m/sec)	2.04	1.47	2.98	2.16
Mean observed U component (m/sec)	1.49	1.40	3.46	2.12
Mean predicted V component (m/sec)	2.79	2.89	3.21	2.96
Mean observed V component (m/sec)	2.30	2.59	3.00	2.63
Standard deviation predicted U component (m/sec)	0.58	0.75	1.34	0.89
Standard deviation observed U component (m/sec)	1.03	1.01	1.86	1.30
Standard deviation predicted V component (m/sec)	0.65	1.23	1.42	1.10
Standard deviation observed V component (m/sec)	1.43	1.71	2.23	1.79
RMSE U component	2.45	2.74	2.15	2.45
RMSE V component	2.34	2.19	3.12	2.55
Index of agreement for wind speed	0.63	0.68	0.70	0.67
Mean observed temperature (°C)	26.83	27.01	30.64	28.16
Mean predicted temperature (°C)	26.90	27.01	30.65	28.19

Table 3b. Statistical summary of the September episode—Domain 2.

Performance Attribute	Sept 3, 1996	Sept 4, 1996	Sept 5, 1996	Mean
Mean wind speed (m/sec)	3.11	2.19	2.18	2.49
Mean predicted wind speed (m/sec)	3.47	3	2.51	2.99
Observed standard deviation	1.82	1.39	1.33	1.51
Predicted standard deviation	2.13	1.85	1.73	1.90
RMSE	2.45	2.01	1.82	2.09
RMSE _U	1.10	0.90	0.81	0.94
RMSE _S	2.19	1.80	1.63	1.87
Mean predicted U component (m/sec)	2.13	1.96	1.89	1.99
Mean observed U component (m/sec)	1.35	1.68	1.46	1.50
Mean predicted V component (m/sec)	1.56	1.83	2.07	1.82
Mean observed V component (m/sec)	1.67	1.54	1.98	1.73
Standard deviation predicted U component (m/sec)	2.34	2.19	2.21	2.25
Standard deviation observed U component (m/sec)	1.87	1.29	1.45	1.54
Standard deviation predicted V component (m/sec)	2.41	1.72	1.91	2.01
Standard deviation observed V component (m/sec)	1.99	1.34	2.01	1.78
RMSE U component	1.7	1.84	1.97	1.84
RMSE V component	1.57	1.76	2.17	1.83
Index of agreement for wind speed	0.77	0.74	0.76	0.76
Mean observed temperature (°C)	24.4	24.08	23.17	23.88
Mean predicted temperature (°C)	25	23.95	23.5	24.15

The mean wind speed for the August episode was overpredicted by 35%. For September, the overprediction was close to 5%; this is due to more data available for that month. For both episodes, temperature data were readily

available and MM5 was within 2% of the observed values for both episodes.

The RMSE values for each episode were less than 2.0. For both cases, the index of agreement was less than 0.8. Figures 5b and 6b show the standard deviation of the wind speed for the August and September episodes.

Finally, our results also show stagnant, weak early morning surface winds on August 13, when the highest ozone peak (137 ppb) occurred in the summer of 1996. The ozone episode of August 13 occurred during a period characterized by a brief period of limited mixing, warm surface and aloft temperatures, and light-to-stagnant surface winds. The predominant synoptic feature on the days prior to the episode was the expansion, intensification, and slow progression eastward of an upper-level ridge of high pressure. On August 13, the 500-mb ridge continued to build and extend, causing the temperatures over El Paso to increase slightly. This aloft warming strengthened the morning inversion. The surface high became much broader and less defined, which caused the near-stagnant morning surface winds. The highest ozone concentration of 137 ppb during 1996 was reached this day at the Chamizal monitoring site. On August 14, the 500-mb ridge continued to move eastward, slightly dissipating from the prior day. This caused the surface pressure to fall west of El Paso, while slightly rising east of El Paso. This resulted in stronger southeasterly and easterly winds in El Paso during this day.

Air was channeled up the river valley to the northwest of El Paso along the west side of the Franklin Mountains. Ozone then reached 87 ppb downwind, at the La Union monitoring site in New Mexico.

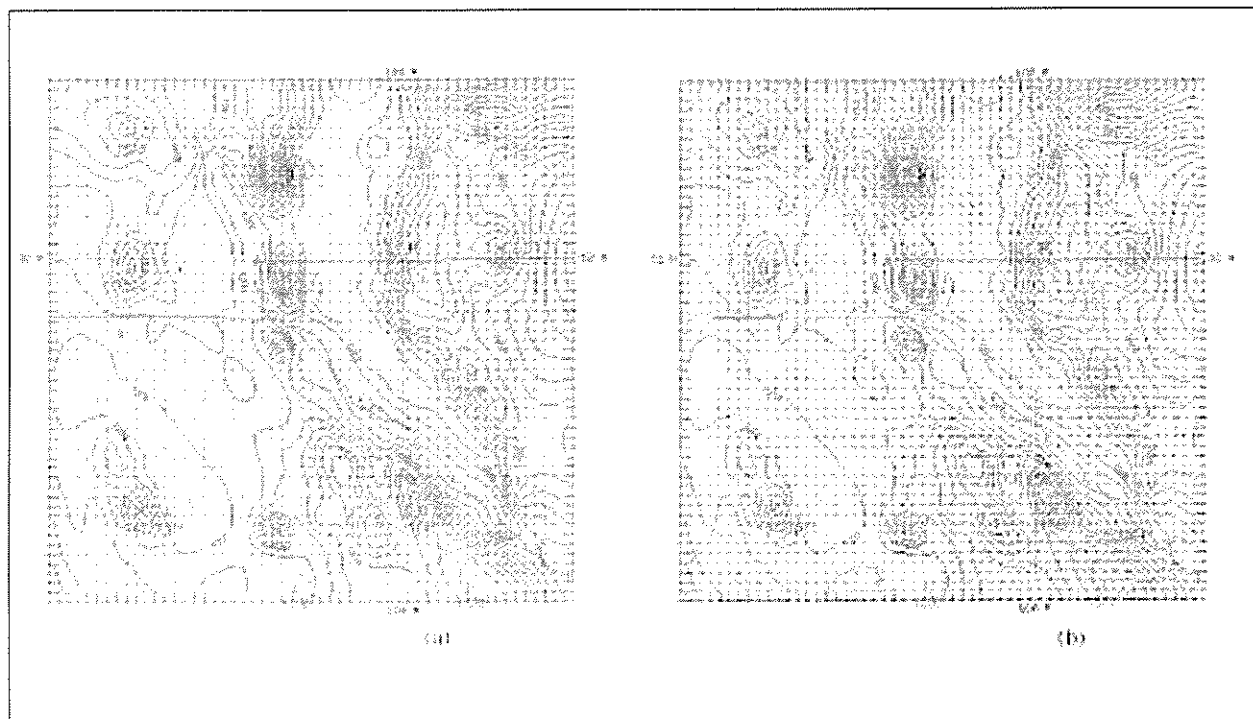


Figure 4. Wind field. (a) August 13, 4:00 a.m. (b) August 13, 4:00 p.m., with terrain elevation contours.

Although slow mixing depth growth (MGR) plays a significant role in producing high ozone concentrations, high ozone concentrations do not occur in El Paso under conditions of moderate-to-strong morning surface winds. The wind has the effect of dispersing horizontally the ozone precursor emissions, which decreases their concentration. Windy days exhibit lower peak ozone concentrations with broader horizontal extent because photochemistry occurs under low precursor concentrations. For example, August 14 and September 3 and 5 all had relatively strong morning winds. August 14 and September 5 had meteorological conditions conducive for high ozone formation, including slow MGRs, except for the winds. The mixing growth rate on August 14 (120 m/hr) was slower than that on August 13, and on September 5 was the same as that on August 13 (150 m/hr). However, the peak downtown ozone concentration on August 14 was only 79 ppb, compared with 137 on August 13. Similarly, peak downtown ozone concentrations on September 5 were only 60 ppb, compared with 137 on August 13. Consequently, we conclude that the dispersion of pollutants by wind played a significant role in the low peak ozone concentrations of August 14 and September 5.

Analysis was also performed per monitoring station in order to get more information on the spatial distribution of meteorological parameters. However, we found a closer correspondence between MM5's statistical domain

averaged parameters and the corresponding observations than in the same comparison per monitoring site. We believe this is because we have not yet achieved the necessary terrain resolution to obtain a close correspondence at the monitoring sites.

Observations show that the winds were slow (0.5–2 m/sec) in the morning hours of the August 12–13, 1996, period in the EPJA. Foothill stations reported downslope winds, especially at Dyer Street, La Union, Franklin Mountain, and 20/30 Club. Stations located at the lower elevations reported near-stagnant conditions with variable wind directions.

Starting from 9:00 a.m. local time, winds were organized and became southeasterly. As the day progressed, their speed was accelerated, reaching 3–5 m/sec on August 12, 2–3 m/sec on August 13, and 4–6 m/sec on August 14. Air was channeled up the river valley to the northwest along the west side of the Franklin Mountains. MM5 also simulated slow winds in the morning hours, replicating down slope winds along the foothills. It is also evident in the MM5's output that the winds were organized and became southeasterly in the afternoon hours of the period. Our results show that channeling of the simulated airflow up the river valley compares well with the observations. Figures 7a–f show a comparison between MM5 results and observed data at La Union Monitoring site for the months of August and September.

CONCLUSIONS

The most significant limitation faced in these efforts was the lack of available data. The results demonstrate the fact that, when more meteorological data is available for input, the model does well, hence the increase in performance from August to September. The RMSE values show that the model is performing well. Our results are in agreement with TNRCC data and with the ozone study performed in 1996 at El Paso.¹ MMS's results led us to conclude that the dispersion of pollutants by wind played a significant role in the low peak ozone concentrations of August 14 and September 5. The 4-km September data show only a 5% error in wind speed. We believe that is an acceptable margin of error for future ozone studies. If it is not seen as acceptable, it could serve as impetus to get more monitoring sites online. The temperature values were in good agreement in all domains. Analysis of the spatial performance of the wind profile shows that the model replicates well the complex circulations of the region. The use of more monitoring stations and better-resolved terrain and land-use data will improve even further the accuracy of the model predictions at the smaller-scale domains. Those data are being derived from observational data by other entities.

For optimum MMS settings, we recommend those used in Table 1. In addition, the Burk PBL scheme should be used in the smaller domains, as the Blackadar may overpredict the temperature at that scale. For the larger scale, the Blackadar is more efficient. Furthermore, we do not recommend the use of cloud cover in the 4-km domain, because at that scale it has no impact. We also recommend

using a fourth domain with a finer grid of 1-km resolution, if well resolved terrain data is available at that scale.

Table 4a. Statistics for the August episode (4-km)—Domain 3.

Performance Attribute	Aug 12, 1996	Aug 13, 1996	Aug 14, 1996	Mean
Mean wind speed (m/sec)	1.15	0.82	1.66	1.21
Mean predicted wind speed (m/sec)	1.98	1.22	1.71	1.64
Observed standard deviation	0.47	0.49	0.54	0.50
Predicted standard deviation	0.83	0.84	0.63	0.77
RMSE	2.13	1.86	1.39	1.79
RMSE _U	0.89	0.81	1.04	0.91
RMSE _S	1.88	1.52	1.03	1.48
Mean predicted U component (m/sec)	1.39	0.93	2.81	1.71
Mean observed U component (m/sec)	1.49	1.40	3.46	2.11
Mean predicted V component (m/sec)	2.13	1.81	2.75	2.23
Mean observed V component (m/sec)	2.30	2.59	3.00	2.63
Standard deviation predicted U component (m/sec)	0.67	0.86	1.56	1.03
Standard deviation observed U component (m/sec)	1.03	1.01	1.86	1.30
Standard deviation predicted V component (m/sec)	0.91	1.66	1.59	1.39
Standard deviation observed V component (m/sec)	1.43	1.71	2.23	1.79
RMSE U component	1.87	1.64	3.56	2.36
RMSE V component	1.96	1.84	3.35	2.39
Index of agreement for wind speed	0.67	0.72	0.74	0.71
Mean observed temperature (°C)	26.83	27.01	30.64	28.16
Mean predicted temperature (°C)	26.9	27.01	30.65	28.19

Table 4b. Statistics for the September episode (4-km)—Domain 3.

Performance Attribute	Sept 3, 1996	Sept 4, 1996	Sept 5, 1996	Mean
Mean wind speed (m/sec)	3.11	2.19	2.18	2.49
Mean predicted wind speed (m/sec)	3.24	2.30	2.34	2.63
Observed standard deviation	1.82	1.39	1.33	1.51
Predicted standard deviation	1.78	1.49	1.24	1.50
RMSE	2.20	1.88	1.50	1.86
RMSE _U	0.98	0.84	0.67	0.83
RMSE _S	1.97	1.68	1.34	1.66
Mean predicted U component (m/sec)	1.48	1.52	1.55	1.52
Mean observed U component (m/sec)	1.35	1.68	1.46	1.50
Mean predicted V component (m/sec)	1.77	1.72	1.88	1.79
Mean observed V component (m/sec)	1.67	1.54	1.98	1.73
Standard deviation predicted U component (m/sec)	0.67	0.86	1.56	1.03
Standard deviation observed U component (m/sec)	1.87	1.29	1.45	1.54
Standard deviation predicted V component (m/sec)	1.93	1.34	1.46	1.58
Standard deviation observed V component (m/sec)	1.99	1.34	2.01	1.78
RMSE U component	1.87	1.54	1.86	1.76
RMSE V component	2.30	1.56	1.93	1.93
Index of agreement for wind speed	0.78	0.79	0.78	0.78
Mean observed temperature (°C)	24.40	24.08	23.17	23.88
Mean predicted temperature (°C)	24.90	24.01	23.65	24.19

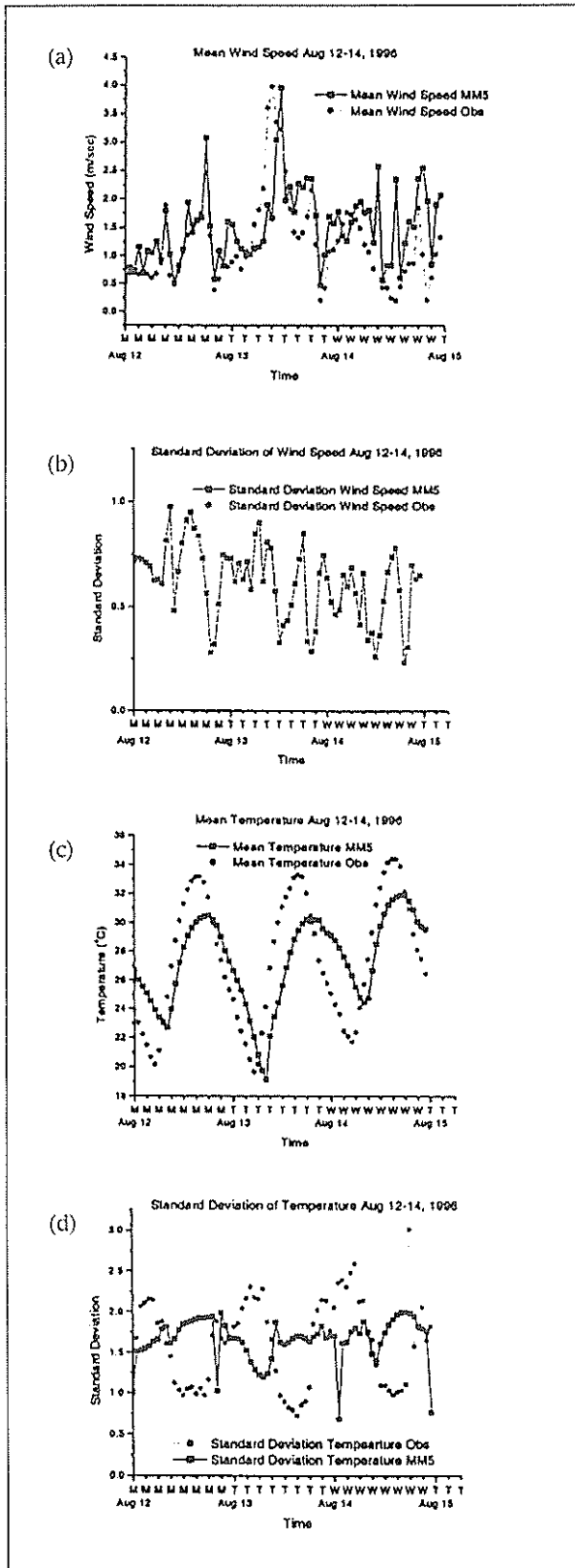


Figure 5. August statistical plots. (a) Mean wind speed. (b) Standard deviation of wind speed. (c) Mean temperature. (d) Standard deviation of temperature.

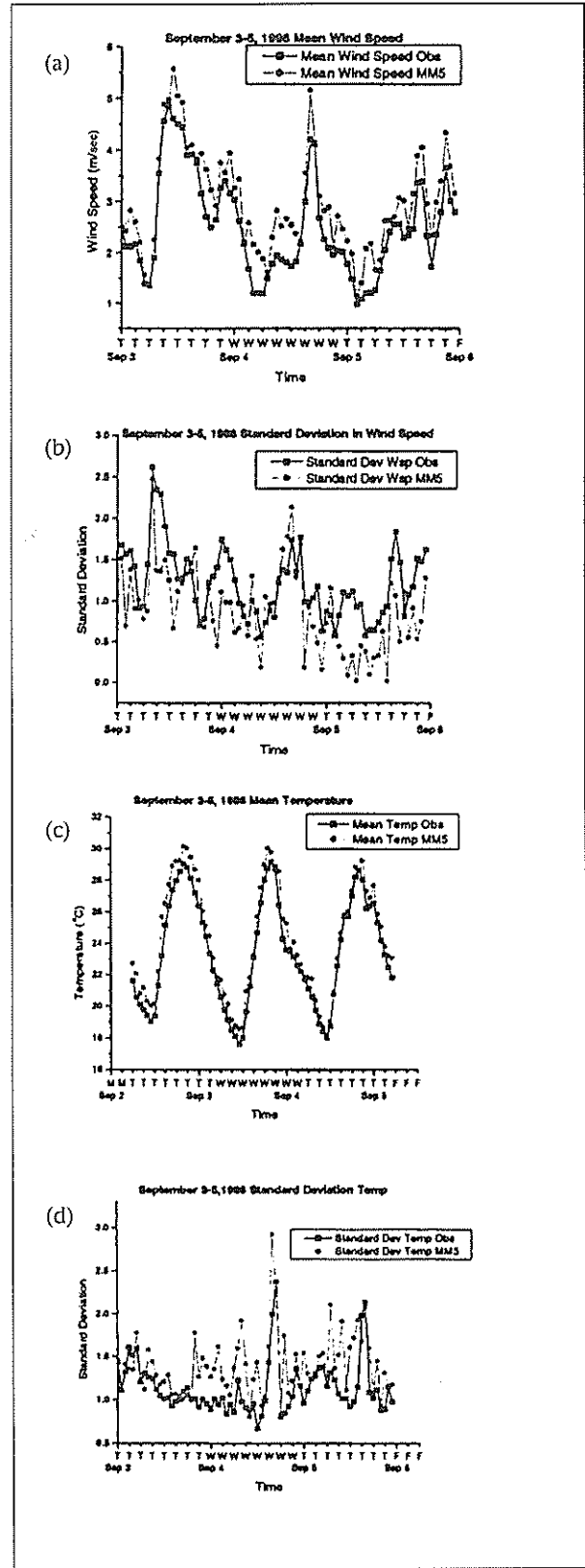


Figure 6. September statistical plots. (a) Mean wind speed. (b) Standard deviation of wind speed. (c) Mean temperature. (d) Standard deviation of temperature.

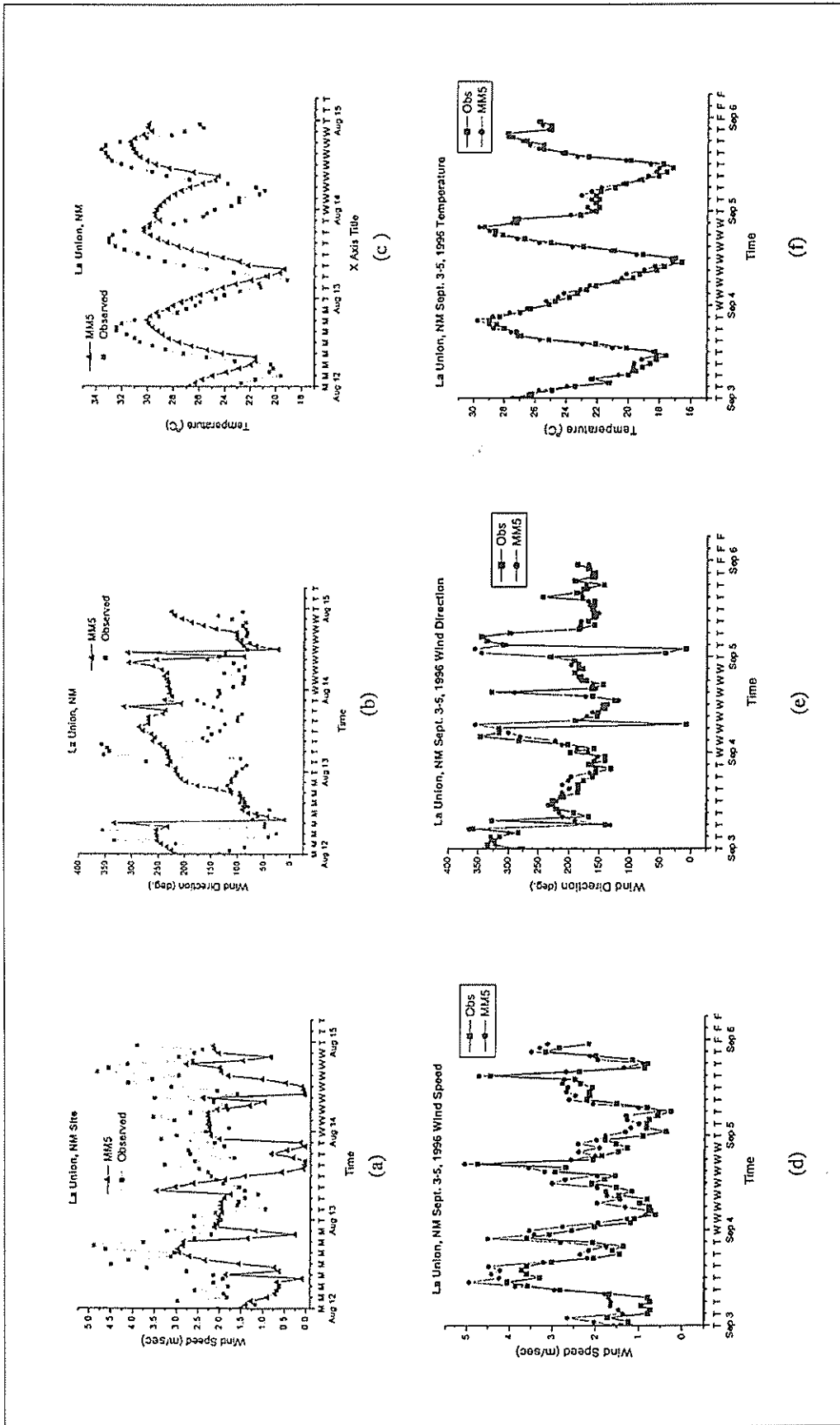


Figure 7. La Union, NM, August 1996: (a) Mean wind speed. (b) Standard deviation of wind speed. (c) Mean temperature. September 1996: (d) Mean wind speed. (e) Standard deviation of wind speed. (f) Mean temperature.

ACKNOWLEDGMENTS

The authors wish to express their gratitude to Saffet Tanrikulu from the Air Resources Board for his invaluable guidance during the course of this project, to the members of the Center for Environmental Research Management for their constant support, to the National Center for Atmospheric Research for allocation of computer time, and to Pete Britenbach from TNRCC and Jim Yarbrough from EPA for providing us with the data and very helpful discussions.

REFERENCES

1. Roberts, P.T.; McDonald, C.P.; Main, H.H.; Dye, T.S.; Coe, D.L.; Haste, T.L. *Analysis of Meteorological and Air Quality Data for the 1996 Paso Del Norte Ozone Study*; U.S. Environmental Protection Agency, Region VI: Dallas, TX, 1997.
2. Grell, et al. Semi-Prognostic Tests of Cumulus Parameterization Schemes in the Middle Latitudes; *Mon. Wea. Rev.* 1991, 119, 5-31.
3. Tesche, T.W.; Haney, J.L.; Causley, M.C. *Photochemical Modeling of Four Areas in Texas, Volume IV: UAM Application for El Paso*; Texas Natural Resources Conservation Commission: Austin, TX, 1991.
4. *El Paso Ozone Nonattainment Areas Base Case Report Modeling Domain/Episode Selection Meteorology/Air Quality*; Texas Natural Resources Conservation Commission: Austin, TX, 1994.
5. *El Paso Ozone Nonattainment Areas Base Case Report Performance Evaluation*; Texas Natural Resources Conservation Commission: Austin, TX, 1994.
6. Randolph, J.E.; Atchison, M.K.; Capuano, M.E.; Emery, C.A.; Yocke, M.A.; Costigan, K.; Tremback, C.; Yarbrough, J.W.; Karp, R.; Hugo, V.; Figuero, P. Meteorological and Photochemical Modeling of Ozone and Carbon Monoxide Episodes for the Paso del Norte Airshed. Part I: Mesoscale Modeling. Presented at the 11th Joint Conference on the Applications of Air Pollution Meteorology with A&WMA, Long Beach, CA, 2000.
7. Emery, C.A.; Yocke, M.A.; Evans, R.J.; Capuano, M.; Costigan, K.; Yarbrough, J.W.; Karp, R.; Hugo, V.; Figuero, P. Meteorological and Photochemical Modeling of Ozone and Carbon Monoxide Episodes for the Paso del Norte Airshed. Part I: Air Quality Modeling. Presented at the 11th Joint Conference on the Applications of Air Pollution Meteorology with A&WMA, Long Beach, CA, 2000.
8. Grell, J. Prognostic Evaluation of Assumptions Used by Cumulus Parameterizations; *Mon. Wea. Rev.* 1993, 121, 764-787.
9. Stauffer, D.R.; Seaman, N.L. Use of Four-Dimensional Data Assimilation in a Limited-Area Mesoscale Model; *Mon. Wea. Rev.* 1990, 119, 734-754.
10. Blackadar. High Resolution Models of the Planetary Boundary Layer. In *Advances in Environmental Science and Engineering*; Pfafflin, Ziegler, Eds.; Gordon and Breich: New York, 1979; pp 50-85.
11. Tesche, T.W.; McNally. *The Use of San Joaquin Valley Meteorological Model in Preparation of a Field Program in the South Coast Air Basin and Surrounding Regions of Southern California*; Report prepared for State of California Air Resources Board by Alpine Geophysics: 1997.
12. Burk, S.D.; Thompson, W.T. A Vertically Nested Regional Numerical Prediction Model with Second-Order Closure Physics; *Mon. Wea. Rev.* 1989, 117, 2305-2324.
13. Willmott, C.J. On the Validation of Models; *Phys. Geography* 1981, 2, 184-194.

About the Authors

Roderick Pearson has a B.S. and an M.S in physics and is currently a doctoral student in the Environmental Science and Engineering Program at the University of Texas at El Paso. Rosa M. Fitzgerald, Ph.D. (corresponding author; e-mail: rfitzger@utep.edu), is an assistant professor in the Physics Department and is affiliated with the Environmental Science and Engineering Ph.D. Program at the University of Texas at El Paso and with the CERM Institute.